Evidence for Superlattice Arrangements in Fluid Phosphatidylcholine/ Phosphatidylethanolamine Bilayers

Kwan Hon Cheng,* Mika Ruonala,# Jorma Virtanen,# and Pentti Somerharju†
*Department of Physics, Texas Tech University, Lubbock, Texas 79409 USA, #Institute of Biomedicine, Department of Medical Chemistry, University of Helsinki, Helsinki, Finland, and #College of Medicine, Department of Radiology, University of California at Irvine, Irvine, California 92717 USA

ABSTRACT Recently, evidence for cholesterol and phosphatidylcholine (PC) molecules to adapt superlattice arrangements in fluid lipid bilayers has been presented. Whether superlattice arrangements exist in other biologically relevant lipid membranes, such as phosphatidylethanolamine (PE)/PC, is still speculative. In this study, we have examined the physical properties of fluid 1-palmitoyl-2-oleoyl-PC (POPC) and 1-palmitoyl-2-oleoyl-PE (POPE) binary mixtures as a function of the POPE mole fraction (X_{PE}) using fluorescence and Fourier transform infrared spectroscopy. At 30°C, i.e., above the T_m of POPE and POPC, deviations, or dips, as well as local data scattering in the excimer-to-monomer fluorescence intensity ratio of intramolecular excimer forming dipyrenylphosphatidylcholine probe in POPE/POPC mixtures were detected at $X_{PE} \approx 0.04$, 0.11, 0.16, 0.26, 0.33, 0.51, 0.66, 0.75, 0.82, 0.91, and 0.94. The above critical values of X_{PE} coincide (within ± 0.03) with the critical mole fractions $X_{HX,PE}$ or $X_{R,PE}$ predicted by a headgroup superlattice model, which assumes that the lipid headgroups form hexagonal or rectangular superlattice, respectively, in the bilayer. Other spectroscopic data, generalized polarization of Laurdan and infrared carbonyl and phosphate stretching frequency, were also collected. Similar agreements between some of the observed critical values of X_{PE} from these data and the $X_{HX,PE}$ or $X_{R,PE}$ values were also found. However, all techniques yielded critical values of X_{PE} (e.g., 0.42 and 0.58) that cannot be explained by the present headgroup superlattice model. The effective cross-sectional area of the PE headgroup is smaller than that of the acyl chains. Hence, the relief of "packing frustration" of PE in the presence of PC (larger headgroup than PE) may be one of the major mechanisms in driving the PE and PC components to superlattice-like lateral distributions in the bilayer. We propose that headgroup superlattices may play a significant role in the regulation of membrane lipid compositions in cells.

INTRODUCTION

In recent years, it has become obvious that considerable heterogeneity in lateral organization, domain formation, of lipids and proteins may exist in biological membranes due to specific and nonspecific lipid-lipid, lipid-protein, and protein-protein interactions (Mouritsen and Biltonen, 1993; Tocanne et al., 1994; Welti and Glaser, 1994). It is believed that formation of these microdomains is relevant to the functioning of cell membranes and is linked to such crucial cellular phenomena as signal transduction, endo- and exocytosis, intracellular lipid and protein sorting, cholesterol efflux, and phospholipase activity (Simons and van Meer, 1988; Bretscher and Munro, 1993; Fielding and Fielding, 1995) as well as regulation of cell membrane lipid compositions (Virtanen, Cheng, and Somerharju, manuscript in preparation).

The molecular interactions responsible for the formation of segregated lipid domains in natural or model lipid membranes are not fully understood. Attractive interactions, e.g., interlipid hydrogen bonding (Hitchcock et al., 1974; Hauser et al., 1981) and hydrophobic effect at the lipid/water interface (Seddon, 1990), have been proposed. Also, repulsive interactions, e.g., steric strain (Somerharju et al., 1985; Chong, 1994; Cheng and Somerharju, 1996) and dipolar interactions (J. Virtanen et al., manuscript in preparation) among headgroup regions, have been suggested. Other interactions, such as hydration (Brown et al., 1986; Gruner, 1992) and intrinsic-curvature-associated packing constraints (Gruner, 1992; Cheng and Somerharju, 1996) at the headgroup and hydrocarbon levels, may also be involved. Repulsive steric interactions at the hydrocarbon level have been proposed to be mainly responsible for the formation of the putative cholesterol or pyrenylacyl superlattices in fluid phosphatidylcholine (PC) host bilayers (Somerharju et al., 1985; Tang and Chong, 1992; Chong, 1994; Tang et al., 1995; Parasassi et al., 1995; Virtanen et al., 1995). However, interactions at the headgroup level that may give rise to the formation of superlattices had not been investigated either theoretically (Virtanen et al., manuscript in preparation) or experimentally until now. Headgroup superlattices could form in bilayers containing two phospholipids that differ significantly in the steric properties of their polar headgroups or when one of the species carries a net charge. In fact, the formation of stoichiometric complexes, or compounds, observed previously in various mixed lipid bi- or monolayer systems (Berclaz and McConnell, 1981; Cunningham et al., 1989; Heimburg et al., 1992; Swamy et al.,

Received for publication 5 March 1997 and in final form 20 June 1997.

Address reprint requests to Dr. Kwan Hon Cheng, Biophysics Lab (Sc-109), Department of Physics, P.O. Box 41051, Texas Tech University, Lubbock, TX 79409-1051. Tel.: 806-742-2992; Fax: 806-742-1182; E-mail: vckhc@ttacs.ttu.edu.

Abbreviations used: diPyr$_n$PC, 1,2-pyrenylacylphosphatidylcholine; E/M, excimer to monomer fluorescence intensity ratio; Laurdan, 2-dimethylamino-6-lauroylnaphthalene; POPC, 1-palmitoyl-2-oleoyl-phosphatidylcholine; POPE, 1-palmitoyl-2-oleoyl-phosphatidylethanolamine.

0006-3495/97/10/1967/10 $2.00

1995; Dibble et al., 1996), could be interpreted as formation of headgroup superlattices in those systems.

PC and phosphatidylethanolamine (PE) are two major phospholipid components of mammalian cell membranes. They differ considerably in their effective sizes, hydration properties, and interhydrogen bonding capability of their polar headgroups (Hitchcock et al., 1974; Brown and Seelig, 1978; Hauser et al., 1981; Brown et al., 1986; Cheng et al., 1986) as well as their intrinsic curvatures (Fenske et al., 1990; Gruner, 1992; Cheng and Somerharju, 1996) pertinent to the effective structure and intermolecular interactions of lipid molecules in membranes. Therefore, it seemed possible that headgroup superlattices could form in mixed bilayers of these lipid species. Accordingly, we have investigated here the physical properties of 1-palmitoyl-2-oleoyl-PC (POPC) and 1-palmitoyl-2-oleoyl-PE (POPE) binary lipid mixtures as a function of composition. POPC and POPE have identical acyl chain composition but differ only in their headgroups. They are therefore an ideal membrane system for investigating the superlattice formation that is solely related to the headgroup interactions. The physical properties of POPE/POPC fluid bilayers were studied by fluorescence spectroscopy employing 1) intramolecular excimer formation probes, dipyrenylphospholipids (Cheng and Somerharju, 1996), that are sensitive to the packing of the acyl chains at well defined depth of the membranes and 2) membrane surface hydration/packing order sensitive probes, Laurdan (2-dimethylamino-6-lauroylnaphthalene) (Parasassi et al., 1994). Parallel and noninvasive Fourier transform infrared spectroscopy (FTIR) measurements that monitored the vibrational properties of the carbonyl and phosphate moieties (Cheng, 1991, 1994) were also carried out.

MATERIALS AND METHODS

Lipids, fluorescent probes, and chemicals

POPC and POPE were purchased from Avanti Polar Lipids (Alabaster, AL) and were found to be over 99% pure based on thin layer chromatography analysis. Dipyrenylacylphosphatidylcholines (diPyr$_n$PCs; n = 6, 8, 10, and 12) were synthesized as described before (Somerharju et al., 1987). DiPyr$_4$PC and Laurdan were purchased from Molecular Probes (Eugene, OR). All solvents were obtained from Merck (Espoo, Finland) and were of the highest purity available.

Preparation of lipid dispersions and hydrated films

The stock solutions containing POPC and POPE in varied ratios were prepared in chloroform and stored at −25°C in the dark. From these stocks, aliquots (100 nmol of total lipid) were drawn and mixed with the fluorescent probes (0.1 nmol for diPyr$_n$PC and 1 nmol for Laurdan) in 300 μl of chloroform. The tubes were placed in a 42°C water bath and the solvent was evaporated under a nitrogen stream. Any residual solvent was then removed by placing the samples under vacuum for at least 5 h. The dry lipid films were subsequently dispersed in buffer (100 mM NaCl/10 mM TES/2 mM EDTA, pH 7.4) at 4°C under rigorous vortexing for 1 min. After more than 24 h of incubation at 4°C, the samples were kept at 35°C for 30 min and then 4°C for another 30 min. This temperature cycling was repeated at least three times. The samples were kept in the dark for at least 12 h at 4°C. Before the fluorescence measurement, the sample was equilibrated at 30°C for 15 min in the dark to stabilize the temperature. The sample temperature was regulated to 30 ± 0.02°C during the measurements. For FTIR measurements, the lipid suspensions were concentrated by centrifugation at 15,000 × g for 20 min. The lipid pellet was applied between two CaF_2 windows separated by a 25-μm Teflon spacer to form a thin hydrated lipid film. The sample was mounted on a thermostatted cell H200 (Wilmad, Buena, NJ). We noted that the temperature cycling procedure appeared to be crucial for obtaining reproducible fluorescence and FTIR data. The gel-to-liquid crystalline phase transition temperatures T_m of neat POPC and POPE membranes are approximately 4 and 26°C (Barenholtz et al., 1976; Small, 1986), respectively. For POPE/POPC mixtures, our fluorescence measurement using diPyr$_{10}$ PC (results not shown) indicated that the T_m shifts from 26°C at X_{PE} = 1.00 to ~21°C at X_{PE} = 0.95. Therefore, POPE/POPC mixtures are in the fluid state at or above room temperature (25°C) for $X_{PE} < 0.95$.

Fluorescence measurements

Most of the fluorescence measurements were performed on a home-built optical multichannel analyzer equipped with a UV-enhanced proximity focused intensified photodiode array IRY-700S detector (Princeton Instrument, Trenton, NJ) attached to a ⅓ m SPEX Minimate 1681 C spectrograph (SPEX Industries, Edison, NJ). A Liconix 4240NB cw UV He-Cd laser (Santa Clara, CA) operating at 325 nm was the excitation source. With this apparatus, a fluorescence spectrum (340–520 nm) of diPyr$_n$PC covering the monomer and excimer bands (Birks et al., 1963) of conjugated pyrene can be obtained in less than 30 ms. Normally, 20–50 spectra were accumulated and the average E/M ratio, defined as the ratio of the intensity of the pyrene excimer emission (centered at 475 nm) to that of the monomer emission (centered at 392 nm) was determined. With this system the uncertainty in E/M is typically ±0.01 (Cheng and Somerharju, 1996).

Similar spectral measurements (380–570 nm) were performed with samples containing Laurdan. The emission spectrum of Laurdan consists of a major peak close to 440 nm (I_B) and a red-shifted shoulder at approximately 490 nm (I_R), which has been attributed to the dipolar solvent relaxation around the excited probe at the lipid/membrane interface (Parasassi et al., 1994). The generalized polarization (G-polarization), defined as $(I_B - I_R)/(I_B + I_R)$, can be used to quantitate the extent of dipolar relaxation of Laurdan (Parasassi et al., 1994).

FTIR measurements

Infrared spectra were recorded with an Analect RFX-40 Fourier transform infrared spectrometer (Laser Precision, Irvine, CA) equipped with a liquid-nitrogen-cooled mercury-cadmium-telluride detector. Typically, 300 interferograms were collected, averaged, and Fourier transformed by standard procedure as described in detail elsewhere (Cheng, 1991, 1994). The overall spectral resolution was better than 0.250 cm^{-1}.

Theoretical predictions of the critical compositions in PE/PC membranes

We have previously derived the equations giving the critical compositions corresponding to different possible superlattice arrangements of lipid molecules in bilayers consisting of 1) pyrene-labeled and unlabeled PC or 2) PC and cholesterol (Virtanen et al., 1988, 1995). In those cases, the phospholipid acyl chains or the cholesterol molecules were considered as the relevant elements of the putative superlattices. However, the same formalism may be applied when analyzing lipid headgroup superlattices. Thus, assuming that the headgroups are hexagonally (HX) or rectangularly (R) arranged, the critical PE mole fractions, $X_{HX,PE}$ or $X_{R,PE}$, respectively,

for a binary system with $X_{PE} < 0.5$ are obtained from the equation:

$$X_{HX,PE} = \frac{1}{a^2 + ab + b^2}$$

or

$$X_{R,PE} = \frac{1}{ab + b^2} \quad X_{PE} < 0.5 \tag{1}$$

where a and b refer to the distance between two proximal guest (PE) elements (headgroups), given in lattice sites along the principal lattice axes (Virtanen et al., 1988). When $X_{PE} > 0.5$, i.e., PC becomes the quest, the equation is transformed to:

$$X_{HX,PE} = 1 - \frac{1}{a^2 + ab + b^2}$$

or

$$X_{R,PE} = 1 - \frac{1}{ab + b^2} \quad X_{PE} > 0.5 \tag{2}$$

Thus the critical mole fractions distribute symmetrically around $X_{PE} = 0.5$; i.e., for each critical $X_{HX,PE}$ or $X_{R,PE}$ there is a critical concentration at $1 - X_{HX,PE}$ or $1 - X_{R,PE}$ (see Table 1). The lateral arrangements of PE (guest) and PC (host) at $X_{HX,PE} = 0.14$ ($a = 2$, $b = 1$) is demonstrated in Fig. 1. Additional details of this headgroup superlattice (HGSL) model will be given elsewhere (Virtanen et al., manuscript in preparation)

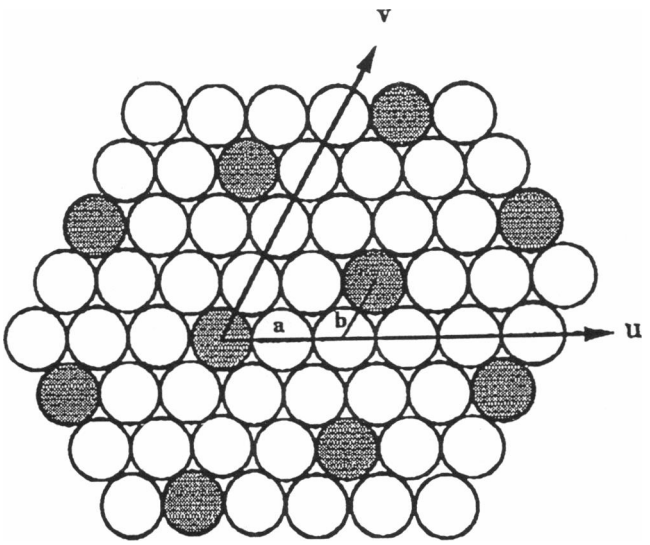

FIGURE 1 The lateral arrangement of the lipid headgroups of PE/PC mixtures at PE mole fraction of 0.143 as predicted by the superlattice model. The bilayer is viewed from above and the PC and PE headgroups are indicated by open and closed circles, respectively. The shape of the symbols emphasizes the assumed effective cross-sectional shape of the headgroups generated by their rapid rotation in the plane of the membrane.

Data analysis, calculations of data scattering, and detection of critical mole fractions

In this study, each spectroscopic data point y_i at the ith PE mole fraction (X_{PE}) represents an average of measurements from three independently prepared, or parallel, samples, and the corresponding standard deviation sd_i is also given. To investigate the general trend of the data, 5-point moving average, y_i^{ma} ($[y_{i-2} + y_{i-1} + y_i + y_{i+1} + y_{i+2}]/5$), is also calculated. In principle, dips and/or kinks in the original spectroscopic data y_i at some particular values of X_{PE} imply "changes" of the physical properties of the lipid membranes at the locations of those "critical" mole fractions.

Besides visual inspection of the primary plots, data-scattering analysis can also be used to detect critical mole fractions (Virtanen et al., 1995). According to the existing superlattice model (Sugar et al., 1994; Virtanen et al., 1995; Virtanen et al., manuscript in preparation), a composition-driven order-to-disorder "phase transition" occurs when the lipid composition approaches a critical one, and the compositional fluctuation is maximal at that "transition". Therefore, data scattering is expected to increase when the composition is close to a critical mole fraction. In this respect, analysis of data scattering should provide additional information on the occurrence of critical mole fractions. For all spectroscopic measurements, a data-scattering parameter y_i^{sc} ($|y_i - y_i^{ma}|$) is used for this purpose (Virtanen et al., 1995). Often, the y_i^{sc} versus X_{PE} data have a severe problem of fluctuations due to the existence of random and systematic errors. To circumvent this problem, two approaches are employed in this study to help locate the critical mole fractions.

The first method is to use the 5-point moving average to smooth the scattering data and evaluate the peaks of the resulting smoothed curve. The other method is more involved and requires a multi-Gaussian fitting procedure using a statistical software package, PeakFit (SPSS, Chicago, IL). Basically, all raw y_i^{sc} versus X_{PE} data were subjected to a Fourier domain filtering to remove the noise in high frequencies with a threshold set at 20% for all data. The peak locations of the filtered data were used as

TABLE 1 Summary of the predicted critical molar fractions $X_{HX,PE}$ and $X_{R,PE}$ in fluid POPE/POPC mixtures according to the HGSL model

Hexagonal				Rectangular			
a	b	X_{PE}	$1 - X_{PE}$	a	b	X_{PE}	$1 - X_{PE}$
				1	1	0.500	0.500
1	1	0.333	0.667	2	1	0.333	0.667
2	0	0.250	0.750	3	1	0.250	0.750
				4	1	0.200	0.800
2	1	0.143	0.857	5	1	0.167	0.833
				2	2	0.125	0.875
3	0	0.111	0.889	0	3	0.111	0.889
2	2	0.083	0.917	1	2	0.083	0.917
3	1	0.077	0.923	5	2	0.071	0.929
4	0	0.062	0.938	2	3	0.067	0.933
5	0	0.040	0.960	4	3	0.048	0.952

See Eqs. 1 and 2 in Materials and Methods.

the seed parameters for the subsequent multi-Gaussian fit to the original y_i^{sc} versus X_{PE} data based on a nonlinear least squares procedure. Initial peaks that were less than twice of the estimated systematic error were considered to be insignificant and thus excluded from fitting. The final fitted peaks are considered significant and provide evidence for the occurrence of critical mole fractions.

RESULTS

Composition-dependent physical properties of POPC/POPE measured by fluorescence and FTIR

Composition-dependent physical properties of fluid POPC/POPE mixtures at 30°C were measured by fluorescence spectroscopy using fluorescent probes, diPyr$_n$PC and Laurdan, and by FTIR spectroscopy without any extrinsic probes. Averages of spectroscopic measurements from three parallel samples and the corresponding standard deviations are given.

Fig. 2 *A* displays the E/M ratio (*upper panel*) of diPyr$_4$PC incorporated in POPE/POPC as a function of X_{PE}. Four dips in E/M ratio at $X_{PE} \approx 0.25, 0.33, 0.67$, and 0.84 are apparent in this plot. More dips are also present at low and high X_{PE}. However, these (putative) dips are so close to each other that they cannot be readily resolved visually. Additional information concerning the identification of critical compositions can be obtained by analyzing data scattering (see Materials and Methods). Fig. 2 *B* shows the plot of data scattering y_i^{sc} as a function of X_{PE} and the smoothed (5-point moving average) scattering curve. The four major dips in E/M ratio now show up as prominent peaks at identical locations in this data-scattering plot. In addition, other scattering peaks at $X_{PE} \approx 0.04, 0.11, 0.16, 0.42, 0.51, 0.56, 0.76, 0.90$, and 0.95 become apparent from the scattering curve. Based on the peaks of the scattering curve, the critical mole fractions at $X_{PE} \approx 0.04, 0.11, 0.16, 0.25, 0.33, 0.51, 0.67, 0.76, 0.84, 0.90$, and 0.95 agree ($\pm 0.01$) with the values of $X_{HE,PE}$ or $X_{R,PE}$ (see Table 1) as predicted by the HGSL model. However, other critical mole fractions, 0.42 and 0.56, do not agree (± 0.03) with any of the values of $X_{HE,PE}$ or $X_{R,PE}$ from the HGSL model. The separation of adjacent PE mole fractions of the samples here is 0.005. Therefore, a 5-point moving average used in data-scattering analysis essentially reflects an effective composition resolution of ± 0.03. In this respect, the number 0.03 is chosen as the comparison threshold between the smoothed scattering peaks and the values of $X_{HE,PE}$ or $X_{R,PE}$. The E/M ratios of other diPyr$_n$PC probes (n = 6, 8, 10, and 12) as a function of X_{PE} around the region of X_{PE} = 0.30–0.40 were also measured (results not shown). Dips at approximately 0.33–0.34 are also found for those diPyr$_n$PC probes.

Fig. 3 *A* displays the G-polarization of Laurdan incorporated in POPE/POPC as a function of X_{PE}. Laurdan has a major emission peak at 440 nm and a red-shifted shoulder (due to dipolar relaxation of excited Laurdan molecules) at 490 nm in fluid-phase lipid membranes (Parasassi et al., 1994). In our PE/PC mixtures, the red-shifted shoulder of Laurdan emission at 490 nm was clearly resolved at low X_{PE}

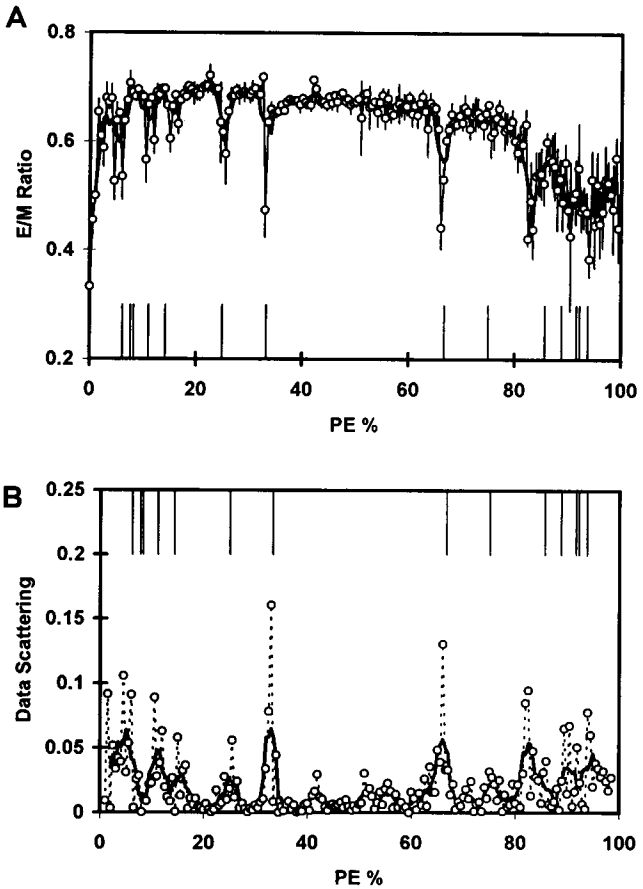

FIGURE 2 (*A*) E/M ratio of diPyr$_4$PC in POPE/POPC mixtures as a function of PE mol % at 30°C. Each data point (○) represents an average of measurements from three parallel samples. Vertical bars on the data points indicate standard deviations. A thick solid line joining the 5-point running averages of the data points is drawn to show the general trend of the data points. (*B*) Data scattering, defined as the absolute value of the scattering (data point − 5-point moving average), as a function of PE mol %. The data-scattering points are connected by broken lines. A smoothed curve (*thick solid line*) using 5-point moving average is also shown to indicate the trend of data scattering. For the purpose of comparing experimental results and theoretical predictions, vertical bars on the lower (*upper panel*) and upper (*lower panel*) x axes represent the locations of the critical mole fractions of PE, $X_{HX,PE}$, as predicted by the headgroup superlattice model (see Materials and Methods). For clarity, values of $X_{R,PE}$ that are similar to values of $X_{HX,PE}$, except at 0.125, 0.200, and 0.500 (see Table 1), are not shown.

but started to decrease with increasing X_{PE}. At $X_{PE} > 0.70$, the red shift became unresolved. This diminishing trend of red-shoulder emission resulted in a global increase in G-polarization as a function of X_{PE}. A clear dip at X_{PE} around 0.11 is clearly found in the plot. In the data-scattering plot (Fig. 3 *B*), two major peaks at $X_{PE} \approx 0.11$ and 0.32 are found in the scattering curve. Other minor peaks at 0.15, 0.19, 0.27, and 0.35 around the neighborhood of these two major peaks are also detected. Some small peaks around 0.43, 0.49, and 0.54–0.58 appear to exist, too. Here the critical mole fractions at 0.11, 0.15, 0.19, 0.27, 0.32, 0.35, and 0.49 agree (± 0.02) with the values of $X_{HE,PE}$ or $X_{R,PE}$ (see Table 1) as predicted by the HGSL model. However,

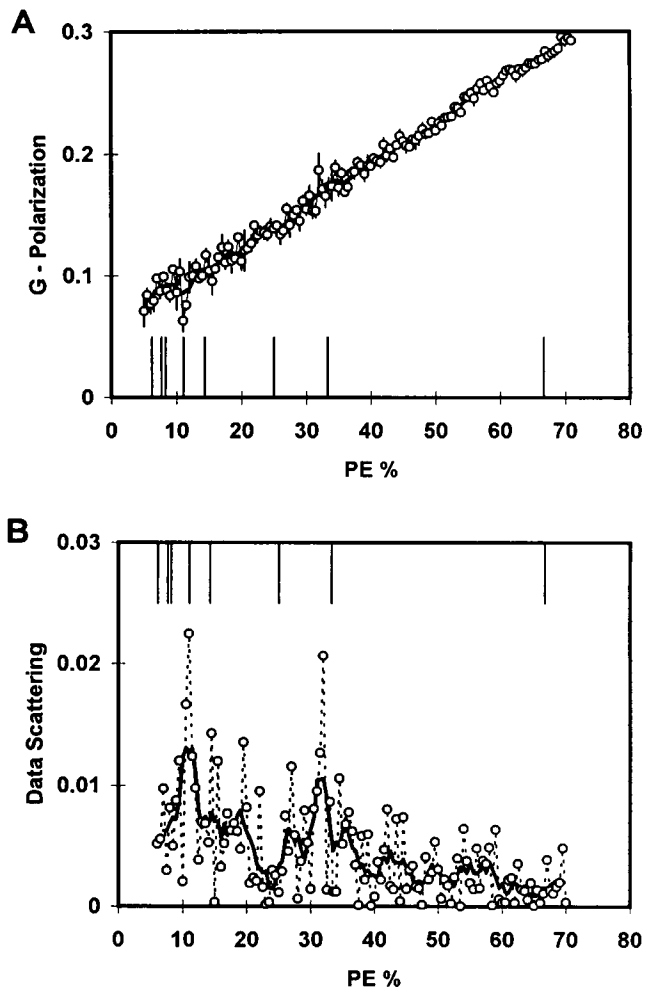

FIGURE 3 (*A*) G-polarization of Laurdan in POPE/POPC mixtures as a function of PE mol % at 30°C. (*B*) Data scattering as a function of PE mol %. See legend of Fig. 2 for data labeling and definitions.

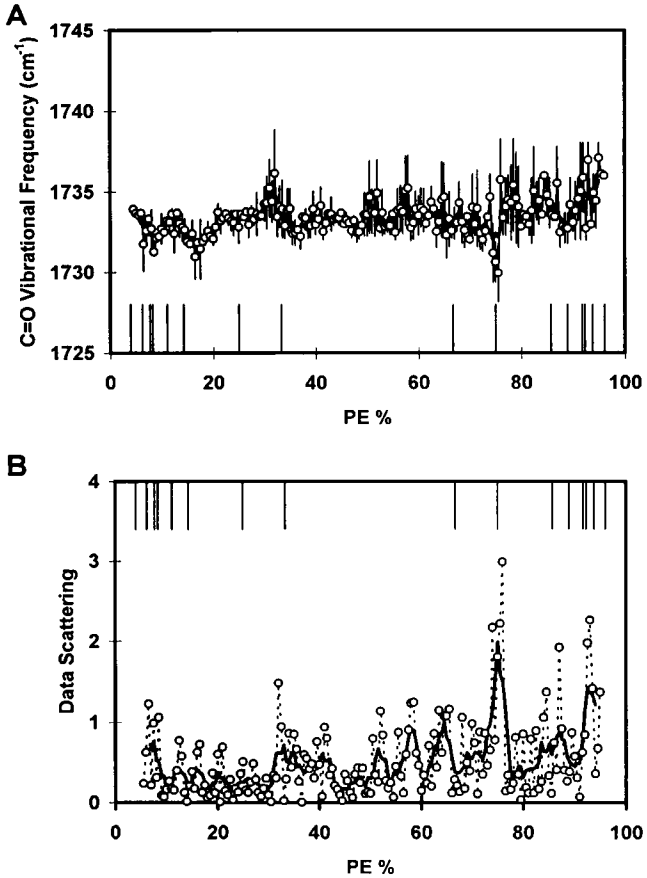

FIGURE 4 (*A*) IR vibrational frequency of interfacial carbonyl (C═O) stretching of native POPE/POPC mixtures as a function of PE mol % at 30°C. (*B*) Data scattering as a function of PE mol %. See legend of Fig. 2 for data labeling and definitions.

the critical mole fractions at 0.42 and 0.54–0.58 do not correspond (±0.03) to any of the $X_{HE,PE}$ or $X_{R,PE}$ values from the HGSL model.

Fig. 4 *A* displays the C═O vibrational frequency of native POPE/POPC mixtures as a function of X_{PE}. Broad dips appear to be present in the plot at $X_{PE} \approx 0.08$, 0.17, 0.36, 0.77, and 0.90. The scattering curve (Fig. 4 *B*) further reveals peaks at approximately 0.07, 0.12, 0.16, 0.20, 0.33, 0.41, 0.52, 0.59, 0.65, 0.75, 0.88, and 0.94. Here the critical mole fractions at 0.07, 0.12, 0.16, 0.20, 0.33, 0.52, 0.75, 0.88, and 0.93 agree (±0.02) with the values of $X_{HE,PE}$ or $X_{R,PE}$ (see Table 1) as predicted by the HGSL model. Again, the critical mole fractions at 0.41 and 0.59 do not correspond (±0.03) to any of the $X_{HE,PE}$ or $X_{R,PE}$ values from the HGSL model.

Fig. 5 *A* displays the asymmetric O═P═O vibrational frequency of native POPE/POPC mixtures as a function of X_{PE} (Cheng, 1994). A global decline in the phosphate vibrational frequency with X_{PE} is evident in the plot. This decline may be related to the change in the conformation/hydration properties near the headgroup region with increasing PE content. A similar decline in the phosphate vibration with PE was also reported in another PE/PC binary system (Cheng, 1991). Dips are found in the plot at $X_{PE} \approx 0.31$ and 0.77. The scattering curve (Fig. 5 *B*) reveals peaks at 0.06, 0.13, 0.19, 0.31, 0.44, 0.51, 0.57, 0.63, 0.69, 0.73, 0.88, and 0.93. Here the critical mole fractions at 0.06, 0.13, 0.19, 0.31, 0.51, 0.69, 0.73, 0.87, and 0.93 agree (±0.02) with the $X_{HE,PE}$ or $X_{R,PE}$ values (see Table 1) as predicted by the HGSL model. However, the critical mole fractions at 0.44, 0.57, and 0.63 do not correspond (±0.03) to any of the values of $X_{HE,PE}$ or $X_{R,PE}$ from the HGSL model.

Detections of critical mole fractions using a multi-Gaussian fitting procedure

A multi-Gaussian fit procedure (see Materials and Methods) was also employed to detect the critical mole fractions. The instrument-related systematic errors of the E/M ratio of diPyr$_4$PC, G-polarization of Laurdan, and IR vibrational frequency bands (C═O and O═P═O) are estimated to be 0.01, 0.0025, and 0.25, respectively. As expected, these

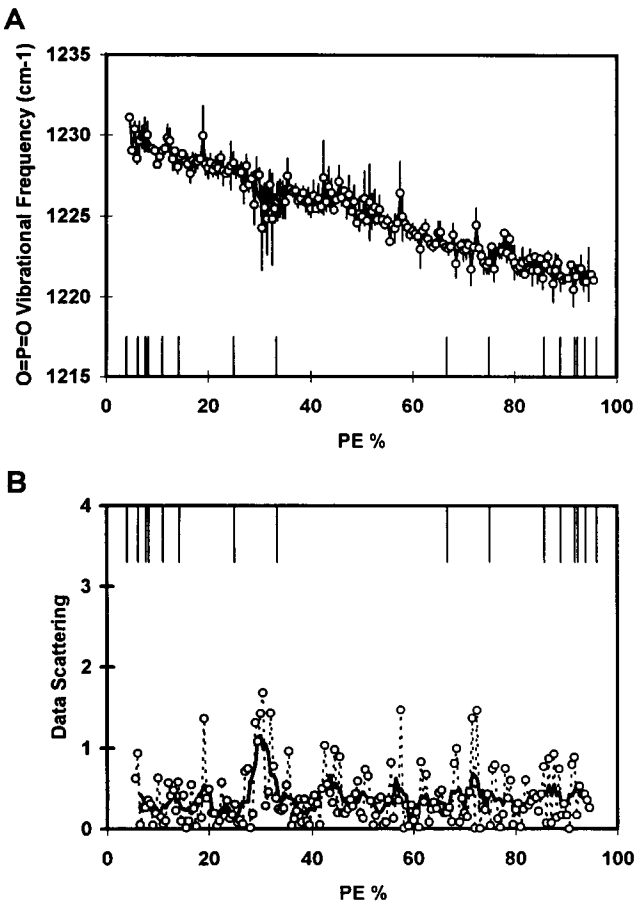

FIGURE 5 (*A*) IR vibrational frequency of headgroup phosphate (O═P═O) stretching of native POPE/POPC mixtures as a function of PE mol % at 30°C. (*B*) Data scattering as a function of PE mol %. See legend of Fig. 2 for data labeling and definitions.

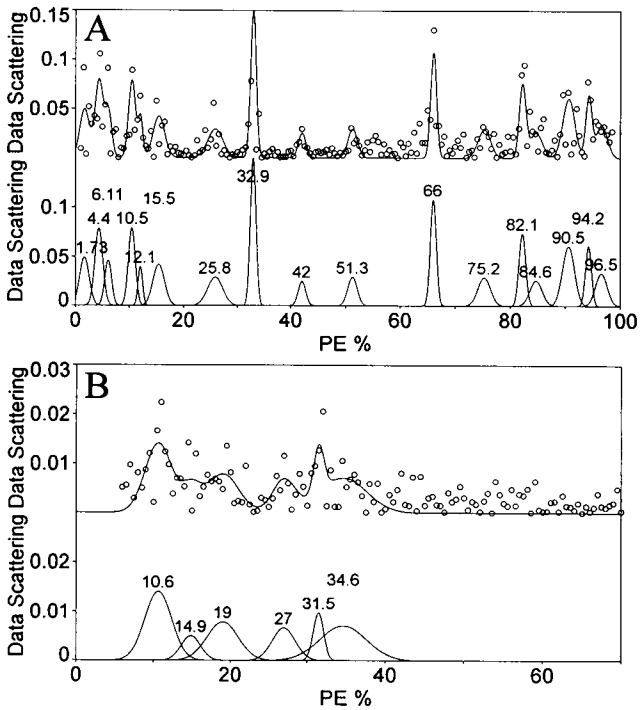

FIGURE 6 Peak analysis of data scattering of fluorescence measurements, E/M ratio of diPyr$_4$PC (*A*) and G-polarization of Laurdan (*B*). The fitted curves and the resolved Gaussian peaks are shown on the upper and lower panels of each graph, respectively. The details of the fitting procedures are given in Materials and Methods and Results.

systematic errors are of similar order of magnitude as the corresponding standard deviations sd_i. The results of the fits (*upper panel*) and the individually resolved Gaussian peaks (*lower panel*) for all the fluorescence and IR measurements are shown in Fig. 6 (E/M and G-polarization) and Fig. 7 (C═O and O═P═O), respectively. The peak locations are also summarized in Table 2. The positions of the peaks provided by this method agree reasonably well with those provided by the more simple averaging method (see above). This method also appears to be able to remove the random noise more effectively than does the averaging method. As shown in Table 2, 15 of 16 (94%) critical values of X_{PE} from diPyr$_4$PC measurements agree with the theoretical mole fractions from the HGSL model (Table 1). The agreements here are within ±0.01, much better than the resolution limit of ±0.03 from scattering analysis. For Laurdan, 6 of 6 (100%) agree (±0.02) with the theoretical fractions. The small scattering peaks at 0.42, 0.49, and 0.58 found in the smoothed scattering curve (see Fig. 3 *B*) were less than the threshold (0.005). Hence they were not resolved in the current analysis. From the less sensitive IR measurements, 13 of 16 (81%) and 8 of 11 (73%) agree (±0.03) with the theoretical fractions for C═O and O═P═O, respectively.

DISCUSSION

Critical compositions in fluid POPC/POPE membrane bilayers

This study provides experimental evidence that the physical properties of fluid PE/PC do not vary smoothly with PE composition, but abrupt, albeit not major, deviations appear to occur at particular critical PE compositions. With the effective resolution of scattering analysis being limited to a mole fraction separation of approximately 0.03, most values of $X_{HX,PE}$ or $X_{R,PE}$, 0.11, 0.14, 0.25, 0.33, 0.50, 0.67, 0.75, and 0.86, were observed by at least two different spectroscopic measurements. However, all techniques yielded critical mole fractions, notably 0.41 and 0.58, that cannot be explained by the current HGSL model.

We propose that deviations in the physical properties of fluid PE/PC occur because the lipid headgroups tend to adapt regular, superlattice-like distributions. This conclusion is supported by the following observations: 1) many of the observed deviations occur at compositions coinciding with the critical compositions $X_{HX,PE}$ and $X_{R,PE}$ predicted by the HGSL model assuming formation of headgroup superlattices and 2) a substantial increase in data scattering often occurs at or close to several predicted critical compositions. The increased scatter is attributed to the predicted compositional fluctuations due to composition-driven order-disorder "phase" transitions close to the critical mole fractions (Sugar et al., 1994; Virtanen et al., 1995).

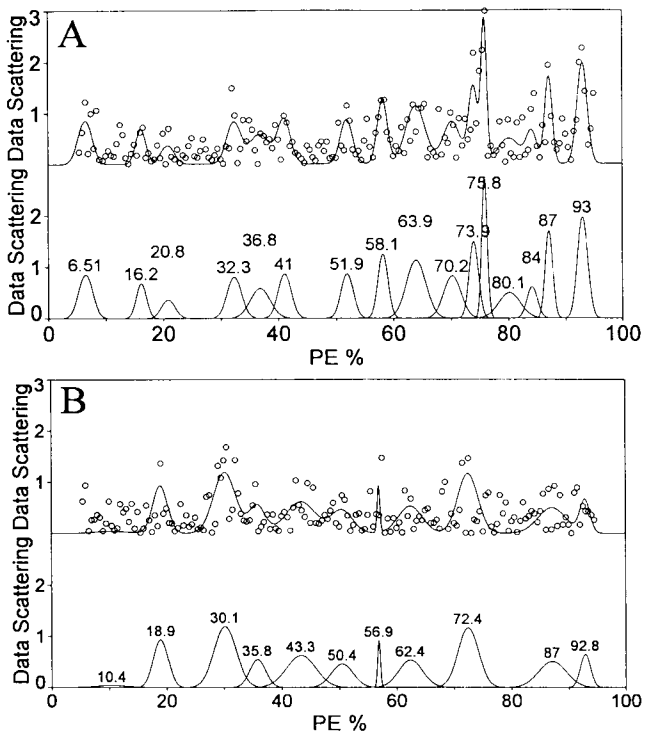

FIGURE 7 Peak analysis of data scattering of IR measurements, C=O (*A*) and O=P=O (*B*). The fitted curves and the resolved Gaussian peaks are shown on the upper and lower panels of each graph, respectively. The details of the fitting procedures are given in Materials and Methods and Results.

Some deviations could not be reliably detected in each experiment. In addition, deviations and/or increased data scatter are observed at compositions that are not predicted by the model (see Table 2). These findings are not unexpected and could relate to one or several of the following factors. First, the changes in membrane physical properties upon transition from one type of superlattice to another are expected to be quite small, because the compositions of subsequent superlattices are often quite similar. Second, the fluorescence properties of the probes and the IR absorption of the native lipids in two consecutive superlattices are probably quite similar, thus decreasing the sensitivity of detection of the transition. Third, the probes could prefer to partition to randomly organized domains, which are predicted to coexist with superlattice domains (Sugar et al., 1994). The relative partitioning coefficients of the probes in organized and random domains are not known. Fourth, there are unavoidable variations in the preparation and measurement of the samples, which, together with the (predicted) increase of data scatter close to the critical compositions (see above), tend to obscure the deviations.

Previously, several investigators have found abrupt changes in the properties of PE/PC bilayers at some of the predicted compositions. Recent studies employing diphenylhexatriene-labeled lipid DPH-PC, monoPyr$_{10}$PC and diPyr$_n$PC (n = 4 and 10) probes indicated a marked deviation in the physical properties of the dilinoleoyl PE/POPC occurs close to X_{PE} of 0.67. (Cheng et al., 1994; Chen and Cheng, 1996). Using FTIR, significant deviation in the C=O vibrational frequency close to 0.67 was also reported in the same dilinoleoyl PE/POPC mixtures (Cheng, 1994). Deviations in the transition enthalpy of dimyristoyl PE (DMPE)/dipalmitoyl PC (DPPC) and DMPE/distearoyl PC (DSPC) bilayers at X_{PE} of approximately 0.33, 0.5, and 0.67 (Blume and Ackermann, 1974) were reported. Also, abrupt changes in the properties of DMPC/DMPE membranes have been observed at X_{PE} close to 0.25 above T_m and close to 0.33 and 0.67 below T_m (Lenz and Litman, 1978). Hunter and Squier (1993) observed many significant deviations in dioleoyl PE/dioleoyl PC membranes at compositions close to those observed in the present study. Finally, Wu and McConnell (1975) have provided evidence for the existence of immiscible fluid "phases" in mixed PE/PC bilayers. These phases could represent domains with distinct PE superlattices (Fig. 1).

Critical compositions have been observed also in other mixed bilayers. A recent study by Swamy et al. (1995) indicated formation of "compounds" with stoichiometries of 1:1 and 1:3 in biotinyl PE/DMPC bilayers. Compounds of 2:1, 1:1, and 1:2 stoichiometries have been suggested to be present in phospholipid/diacylglycerol bilayers below and even above the gel-to-liquid phase transition (Heimburg et al., 1992; Dibble et al., 1996). Although compound formation could indeed be responsible for the observed critical compositions, it is somewhat difficult to see how specific attractive interactions (such as hydrogen bonding) would allow for the formation of compounds of different stoichiometries. The superlattice model, which is based on nonspecific repulsive interactions (see below), does not suffer from this drawback as it intrinsically allows for multiple critical compositions.

Forces responsible for the formation of superlattices in PC/PE bilayers

As discussed by Hauser et al (1981), the minimal cross-sectional area of the (hydrated) headgroup of PC is approximately 63 Å^2 (Janiak et al., 1979). This exceeds markedly the combined minimal cross-sectional area of two all-*trans* acyl chains, i.e., 38–40 Å^2 (Small, 1986). Despite that the effective cross-sectional area of conformationally disordered acyl chains is considerably higher, approximately 50 Å^2 (Hauser et al, 1981), it is obvious that the discrepancy between the headgroup and acyl chain cross-sectional areas is not eliminated even in fluid membranes. Therefore, packing of the molecules in neat, liquid-crystalline PC bilayers may be considered constrained, or "frustrated".

Neat, liquid-crystalline bilayers of unsaturated PE are also often frustrated because the effective cross-sectional area of the headgroup is now smaller than that of the two acyl chains (Hauser et al., 1981; Seddon, 1990; Gruner, 1992). Therefore, when PC and PE are mixed, a less strained bilayer should result because of the complementary

TABLE 2 Comparison of critical mole fractions X_{PE} from fluorescence and IR spectroscopic measurements with $X_{HX,PE}$ or $X_{R,PE}$ values predicted by HGSL model

$X_{HX,PE}$ or $X_{R,PE}$	diPyr$_4$PC	Laurdan	C=O	O=P=O
0.04–0.08^{H,R}	0.04, 0.06	NA	0.07	
0.11–0.13^{H,R}	0.11, 0.12	0.11		0.10
0.14^{H}, 0.17^{R}	0.16	0.15	0.16	
0.20^{R}		0.19	0.21	0.19
0.25^{H,R}	0.26	0.27		
0.33^{H,R}	0.33	0.32, 0.35	0.32	0.30, 0.36
			0.37*	
	0.42*		0.41*	0.43*
0.50^{R}	0.51		0.52	0.50
			0.58*	0.57*
				0.62*
0.67^{H,R}	0.66		0.64, 0.70	
0.75^{H,R}	0.75	NA	0.74, 0.76	0.72
0.80^{R}			0.80	
0.83^{R}, 0.86^{H}	0.82, 0.85	NA	0.84, 0.87	0.87
0.87–0.89^{R,H}	0.91, 0.94, 0.97	NA	0.93	0.93

The critical mole fractions are identified from the peaks of multi-Gaussian fit to the scattering data (see Materials and Methods). Similar critical mole fractions are also detected using a more direct method of the peaks of smoothed data scattering curve. Superscripts H and R denote $X_{HX,PE}$ and $X_{R,PE}$, respectively, from the HGSL model (see Table 1). NA, not available.

*Critical values of X_{PE} that do not agree (± 0.03) with $X_{HX,PE}$ or $X_{R,PE}$ values.

"shapes" of PE and PC. The relief of bilayer frustration is expected to be maximal at a constant composition when the PE and PC molecules adapt an even or regular distribution (see also Virtanen et al., 1995). This phenomenon could be, at least in part, responsible for the formation of microdomains with regular, superlattice-like arrangements in PE/PC bilayers. Another contributing factor could be the possible repulsion between PC headgroups. Theoretical studies (Stigter and Dill, 1988; Dill and Stigter, 1988) indicated that the choline moiety of PC tends to be slightly inclined toward the hydrocarbon phase, thus creating a dipole that causes a strong repulsion between PC headgroups. In accordance with the above considerations, the conformational order of the acyl chains in PC bilayers is known to increase markedly upon addition of PE (Cullis et al., 1986; Fenske et al, 1990; Chen et al., 1992), obviously because the smaller phosphoethanolamine headgroup allows a tighter lateral packing of the acyl chains. This conclusion is strongly supported by the finding that the transition enthalpy of 1:1 mixtures of DMPE and DSPC or DMPE and DPPC is remarkably higher than that of the neat PC or PE bilayer. Importantly, tighter packing of the acyl chains in mixed bilayers should also increase the lateral order, which in turn should favor the formation of headgroup superlattices. The superlattice model requires that the repulsive interactions between similar molecules extend beyond nearest neighbors. That this is feasible is indicated by the fact that addition of less than 10 mol % of dihexadecyl PC is required to stabilize dihexadecyl PE bilayers toward frustration-induced transition to the H_{II}-state (Hing and Shipley, 1995).

Mammalian cell membranes typically contain a significant amount of cholesterol. Therefore, it is relevant to know whether the critical mole fractions in POPE/POPC may also occur in the presence of cholesterol. Our preliminary study (results not shown) shows that addition of 50 mol % cholesterol to the PE/PC bilayers does not abolish the deviation at X_{PE} of 0.33, thus indicating that cholesterol does not interfere with the formation of the headgroup superlattices. This observation is also supported by a recent theoretical study (Virtanen and Somerharju, unpublished results) indicating that the presence of cholesterol molecules should favor superlattice-like organization of the headgroups.

Physiological significance of headgroup-dependent phospholipid superlattices

There is an intriguing possibility that lipid superlattices play a pivotal role in the regulation of membrane lipid compositions (Virtanen et al., 1995). This suggestion is based on the following predicted properties of membranes containing lipid superlattices. First, the critical compositions represent local energy minimum states of the bilayer (Sugar et al., 1994). Hence any deviations from these critical compositions will be energetically unfavorable. Thus these energy minima could provide well defined "set points" (analogous to notches in a tuneable control knob) for the regulatory system. Second, a minor deviation from the critical concentrations will lead to an order/disorder phase transition. Such a transition represents a major change in physical properties of the membrane that control the activity of the key enzymes of phospholipid synthesis by affecting their conformations or lateral distributions, e.g., aggregation/desegregation. The remarkable cholesterol concentration dependency of the activity of the human erythrocyte glucose transporter (Carruthers and Melchior, 1985) could be an example of such a regulatory effect of membrane lateral order. We have

recently found that the previously established phospholipid compositions of the erythrocyte membrane, as a whole or at the level of the individual leaflets, coincide surprisingly well with critical compositions predicted by the superlattice model (Virtanen et al., submitted for publication). This study strongly supports the composition-controlling role of lipid superlattices.

Several authors have suggested that cells may regulate their lipid composition so as to maintain their membranes in the state of phase transition (Melchior et al., 1972; Ashe and Steim, 1971; Shimshick and McConnell, 1973). As the membrane compressibility is maximal at the phase transition, this condition is expected to be optimal for integral membrane enzymes undergoing conformational changes during their catalytic cycle (Shimshick and McConnell, 1973; Eklund et al., 1992). The coexistence of domains with different lipid superlattices (or random distribution), as predicted by the superlattice model (Somerharju et al., 1985; Sugar et al., 1994), would represent a state that is analogous to a "phase transition" and would thus provide the same benefits, while avoiding the problem of explaining how a phase transition would be generated in cellular membranes, e.g., in the intracellular membranes of mammalian cells, which typically lack lipid melting around physiological temperature. Finally, lipid superlattices could be involved in many other physiologically important functions, such as protein and lipid sorting, cell-cell interactions, and transmembrane signal transduction, and will be discussed in more detail elsewhere (Virtanen and Somerharju, submitted for publication).

The skillful technical assistance of Digala Kulawansa, Tarja Grundström, and Titta Tapiola is gratefully acknowledged.

This work was supported by grants from the Robert A. Welch Research Foundation (D-1158) to K.H.C. and from the Finnish Academy and Sigrid Juselius Foundation to P.S.

REFERENCES

Ashe, G. B. and J. M. Steim, 1971. Membrane transitions in Gram-positive bacteria. *Biochim. Biophys. Acta.* 233:810–818.

Barenholtz, Y., J. Suurkuusk, D. Mountcastle, T. E. Thompson, and R. L. Biltonen. 1976. A calorimetric study of the thermotropic behavior of aqueous dispersions of natural and synthetic sphingomyelins. *Biochemistry.* 15:2441–2447

Berclaz, T. and H. M. McConnell. 1981. Phase Equilibria in binary mixtures of dimyristoylphosphatidylcholine and cardiolipin. *Biochemistry.* 20:6635–6640.

Birks, J. B., D. J. Dyson, and I. H. Munro. 1963. "Excimer" fluorescence II. Lifetime studies of pyrene solutions. *Proc. R. Soc. Lond.* 275: 575–588.

Blume, A. and T. Ackermann. 1974. A calorimetric study of the lipid phase transitions in aqueous dispersions of phosphorylcholine-phosphorylethanolamine mixtures *FEBS Lett.* 43:71–74.

Bretscher, M. S. and S. Munro. 1993. Cholesterol and Golgi apparatus. *Science.* 261:1280–1281.

Brown, M. F. and J. Seelig. 1978. Influence of cholesterol on the polar region of phosphatidylcholine and phosphatidylethanolamine bilayers. *Biochemistry.* 17:381–384.

Brown, P. M., J. Steers, S. W. Hui, P. L. Yeagle, and J. R. Silvius. 1986. Role of head group structure in the phase behavior of amino phospholipids. 2. Lamellar and nonlamellar phases of unsaturated phosphatidylethanolamine analogues. *Biochemistry.* 25:4259–4267.

Chen, S., K. H. Cheng, and B. W. van der Meer. 1992. Quantitation of lateral stress in lipid layer containing nonbilayer preferring lipids by frequency-domain fluorescence spectroscopy. *Biochemistry.* 31: 3759–3788.

Chen, S. and K. H. Cheng. 1996. Detection of membrane packing defects by time-resolved fluorescence depolarization. *Biophys. J.* 71:878–884.

Cheng, K. H., J. R. Lepock, S. W. Hui, and P. L. Yeagle. 1986. The role of cholesterol in the activity of reconstituted Ca-ATPase vesicles containing unsaturated phosphatidylethanolamine. *J. Biol. Chem.* 261: 5081–5087.

Cheng, K. H. 1991. Infrared study of the polymorphic phase behavior of dioleoylphosphatidylethanolamine and dioleoylphosphatidylcholine mixtures. *Chem. Phys. Lipids.* 60:119–125.

Cheng, K. H. 1994. Infrared study of bilayer stability behavior of binary and ternary mixtures containing unsaturated phosphatidylethanolamine. *Chem. Phys. Lipids.* 70:43–51.

Cheng, K. H., P. Somerharju, and I. P. Sugar. 1994. Detection and characterization of the onset of bilayer packing defects by nanosecond-resolved intramolecular excimer fluorescence spectroscopy. *Chem. Phys. Lipids.* 74:49–64.

Cheng, K. H. and P. Somerharju. 1996. Effects of unsaturation and curvature on the transverse distribution of intramolecular dynamics of dipyrenyl lipids. *Biophys. J.* 67:914–921.

Chong, P. L-G. 1994. Evidence for regular distribution of sterols in liquid crystalline phosphatidylcholine bilayers. *Proc. Natl. Acad. Sci. USA.* 91:10069–10073.

Carruthers, A. and D. L. Melchior. 1985. Transport of alpha- and beta-D-glucose by the intact human red cell. *Biochemistry.* 24:4244–4250.

Cullis, P. R., M. J. Hope, and C. P. S. Tilcock. 1986. Lipid polymorphism and the roles of lipids in membranes. *Chem. Phys. Lipids.* 40:127–144.

Cunningham, B. A., T. Tsujita, and H. L. Brockman. 1989. Enzymatic and physical characterization of diacylglycerol-phosphatidylcholine interactions in bilayers and monolayers. *Biochemistry.* 28:32–40.

Dill, K. E. and D. Stigter. 1988. Lateral interactions among phosphatidylcholine and phosphatidylethanolamine headgroups in phospholipid monolayers and bilayers. *Biochemistry.* 27:3446–3453.

Dibble, A. R. G., A. K. Hinderliter, J. J. Sando, and R. L. Biltonen. 1996. Lipid lateral heterogeneity in phosphatidylcholine/phosphatidylserine/diacylglycerol vesicles and its influence on protein kinase C activation. *Biophys. J.* 71:1877–1890.

Eklund, K., J. A. Virtanen, P. K. J. Kinnunen, J. Kasurinen, and P. Somerharju. 1992. Conformation of phosphatidylcholine in neat and cholesterol containing liquid crystalline bilayers. *Biochemistry.* 31: 8560–8565.

Fenske, D. B., H. C. Jarrell, Y. Guo, and S. W. Hui. 1990. Effects of unsaturated phosphatidylethanolamine on the chain order profile of bilayer at the onset of hexagonal phase transition. A 2H NMR study. *Biochemistry.* 29:11222–11229.

Fielding, P. E. and C. J. Fielding. 1995. Plasma membrane caveolae mediate the efflux of cellular free cholesterol. *Biochemistry.* 34: 14288–14292.

Gruner, S. M. 1992. Nonbilayer lipid phases. *In* The structure of biological membranes. P. L. Yeagle, editor. CRC Press, Boca Raton, FL. 211–250.

Hauser, H., I. Pascher, R. H. Pearson, and S. Sundell. 1981. Preferred conformation and molecular packing of phosphatidylethanolamine and phosphatidylcholine. *Biochim. Biophys. Acta.* 650:21–51.

Heimburg, T., U. Würtz, and D. Marsh. 1992. Binary phase diagram of hydrated dimyristodylglycerol-dimyristoylphosphatidylcholine mixtures. *Biophys. J.* 63:1369–1378.

Hitchcock, P. B., R. Mason, K. M. Thomas, and G. G. Shipley. 1974. Structural chemistry of 1,2 Dilauroyl-dl-phosphatidylethanolamine: molecular conformation and intermolecular packing of phospholipids. *Proc. Natl. Acad. Sci. USA.* 71:3036–3040.

Hing, F. S. and G. G. Shipley. 1995. Molecular interactions of ether-linked phospholipids. *Biochemistry.* 34:11904–11909.

Hunter, G. W. and T. C. Squier. 1993. Influence of phosphatidylethanolamines on bilayer structure. *Biophys. J.* 64:A68.

Janiak, M. J., D. M. Small, and G. G. Shipley. 1979. Temperature and compositional dependence of the structure of hydrated dimyristoyl lecithin. *J. Biol. Chem.* 254:6068–6078.

Lentz, B. R. and B. J. Litman. 1978. Effect of Head group on phospholipid mixing in small, unilamellar vesicles: Mixtures of Dimyristoylphosphatidylcholine and Dimyristoylphosphatidylethanolamine. *Biochemistry.* 17:5537–5543.

Melchior, D. L. and J. M. Steim. 1972. Lipid-associated thermal events in biomembranes. *Prog. Surface Membr. Sci.* 13:211–296.

Mouritsen, O. G. and R. L. Biltonen. 1993. *In* Protein-Lipid Interactions. A. Watts, editor. Elsevier Scientific Publishers, Ireland. 1–39.

Parasassi, T., M. D. Stefano, M. Loiero, G. Ravagnan, and E. Gratton. 1994. Cholesterol modifies water concentration and dynamics in phospholipid bilayers: a fluorescence study using Laurdan Probe. *Biophys. J.* 60:179–189.

Parasassi, T., A. M. Giusti, M. Raimondi, and E. Gratton. 1995. Abrupt modifications of phospholipid bilayer properties at critical cholesterol concentrations. *Biophys. J.* 68:1895–1902.

Seddon, J. M. 1990. Structure of the inverted hexagonal (HII) phase and nonlamellar transitions of lipids. *Biochim. Biophys. Acta.* 1031:1–69.

Simons, K. and G. van Meer. 1988. Lipid sorting in epithelial cells. *Biochemistry.* 27:6197–6202.

Shimshick, E. J. and H. M. McConnell. 1973. Lateral phase separations in phospholipid membranes. *Biochemistry.* 12:2351–2360.

Small, D. M. 1986. The physical chemistry of lipids. *In* Handbook of Lipid Research. D. K. Hanaham, editor. Plenum Press, New York. 97–143.

Somerharju, P., J. A. Virtanen, K. K. Eklund, P. Vainio, and P. K. J. Kinnunen. 1985. 1,Palmitoyl-2-pyrenedecanonyl glycerophospholipids as membrane probes: evidence for regular distribution in liquid crystalline phosphatidylcholine. *Biochemistry.* 24:2773–2781.

Somerharju, P., D. van Loon, and K. W. A. Wirtz, 1987. Determination of acyl-chain specificity of bovine liver phosphatidylcholine transfer protein. Application of pyrene-labeled phosphatidylcholine species. *Biochemistry.* 26:7193–7199.

Stigter, D. and K. A. Dill. 1988. Lateral interactions among phospholipid head groups at the heptane/water interface. *Langmuir.* 4:200–209.

Sugar, I. P., D. Tang, and P. L.-G. Chong. 1994. Monte Carlo simulation of lateral distribution of molecules in a two-component membrane. Effect of long-range repulsive interactions. *J. Phys. Chem.* 98: 7201–7210.

Swamy, M. J., U. Würz, and D. Marsh. 1995. Phase polymorphism, molecular interactions, and miscibility of binary mixtures of dimyristoyl-N-biotinylphosphatidylethanolamine with dimistoylphosphatidylcholine. *Biochemistry.* 34:7295–7302.

Tang, D. and P. L.-G. Chong. 1992. E/M dips. Evidence for lipid regular distributioned into hexagonal super-lattices in pyrene-PC/DMPC binary mixtures of specific concentrations. *Biophys. J.* 63:903–910.

Tang, D., B. W. Van der Meer, and S.-Y. Chen. 1995. Evidence for a regular distribution of cholesterol in phospholipid bilayers from diphenylhexatriene fluorescence. *Biophys. J.* 68:1944–1951.

Tocanne, J-F., L. Cezanne, A. Lopez, B. Piknova, V. Schram, J-F. Tournier, and M. Welby. 1994. Lipid domains and lipid/protein interactions in biological membranes. *Chem. Phys. Lipids.* 73:139–158.

Virtanen, J. A., P. Somerharju, and P. K. J. Kinnunen. 1988. Prediction of patterns for regular distribution of soluted guest molecules in liquid crystalline phospholipid membranes. *J. Mol. Electron.* 4:233–236.

Virtanen, J. A., M. Ruonala, M. Vauhkonen, and P. Somerharju. 1995. Lateral organization of liquid-crystalline cholesterol-dimyristoyl phosphatidylcholine bilayers. Evidence for domains with hexagonal and center rectangular cholesterol superlattice. *Biochemistry.* 34: 11568–11581.

Welti, R. and M. Glaser. 1994. Lipid domains in model and biological membranes. *Chem. Phys. Lipids.* 73:121–137.

Wu, S. H-W. and H. M. McConnell. 1975. Phase separations in phospholipid membranes *Biochemistry.* 14:847–854.